Structural network topology correlates to cognitive impairment and iPTH level in End-stage renal disease patients with peritoneal dialysis

Longsheng Wang
the Second Hospital of Anhui Medical University
Liwei Zou
Anhui Medical University
Hanqiu Wu
the Second Hospital of Anhui Medical University
Yanqi Shan
the Second Hospital of Anhui Medical University
Ru Zhao
the Second Hospital of Anhui Medical University
Guiling Liu
the Second hospital of Anhui Medical University
Fangbiao Tao
Anhui Medical University
Suisheng Zheng
Ping An Healthcare Diagnostics Center
Xijun Gong (gongxj0306@sina.com)
the Second Hospital of Anhui Medical University

Research article

Keywords: end-stage renal disease, secondary hyperparathyroidism, structural connectivity, topological organization, network

Posted Date: April 24th, 2019

DOI: https://doi.org/10.21203/rs.2.9318/v1

Abstract

Objective: The burden of cognitive impairment in end-stage renal disease (ESRD) undergoing peritoneal dialysis received more attention, which associated with hospitalization, mortality and quality of life. We aimed to assess the topological alterations of brain white matter structural network in ESRD and the correlation between network metrics with Montreal Cognitive Assessment scores and clinical data. Methods: The study included 25 ESRD patients with secondary hyperparathyroidism (SHPT group), 25 patients without SHPT (Non-SHPT group) and 25 healthy controls (HC group) of comparable age and sex. Cognitive function was assessed using Montreal Cognitive Assessment. WM structural network constructed by diffusion tensor imaging and deterministic tractography method, and then used graph theoretical approaches to investigate alterations in the global and regional properties of the WM network in these participants. Results: ESRD patients showed cognitive impairment compared to HC and SHPT patients was lower cognitive scores than Non-SHPT patients. The global topological organization and local efficiency of WM network was significantly disrupted in SHPT but not in Non-SHPT patients, as compared with HC group. Moreover, lower regional efficiency was found in ESRD patients mainly distributed in the frontal and parietal cortices. In addition, association was found between iPTH, shortest path length and cognitive impairment, and iPTH level was negatively correlated with small-worldness by two indexes normalized clustering coefficient and normalized shortest path length. Conclusion: The present study indicated that brain structural connectome in ESRD patients with high iPTH level was disrupted as cognitive impairment and it has the potential connectome-based biomarkers for early detection.

Introduction

Chronic kidney disease (CKD) is a substantial global health problem. There are approximately 571000 patients for end-stage renal disease (ESRD) receive treatment in United States, while nearly 270000 patients with ESRD undergo hemodialysis in China[1, 2]. Cognitive impairment has received more attention in ESRD patients because its prevalence approximately of 30%-60%[1, 3, 4]. The cognitive impairment is associated with adverse outcomes and decreased quality of life[5, 6].

Cerebrovascular disease, anemia, uremic toxins, and secondary hyperparathyroidism (SHPT) have been reported as major causes of cognitive impairment in CKD patients[7-10]. SHPT characterized by high parathyroid hormone (PTH) levels, normal/low calcium levels and concurrent decrease in vitamin D levels. There is evidence from studies supported that PTH levels may be related with increased risk of cognitive decline and incident dementia[11, 12]. However, the pathophysiology of cognitive impairment in ESRD patients with SHPT is still unclear.

Neuroimaging has been established as a reliable tool for assess the neuropathologic mechanism of cognitive impairment in patients with ESRD[13, 14]. Resting-state functional magnetic resonance imaging (rs-fMRI) showed that patients with ESRD have lower ALFF values and abnormal brain functional connectivity in default mode network (DMN) regions when compared with healthy controls[15]. Recent

studies have revealed that whole brain white matter (WM) connectivity can be reconstructed with diffusion tensor imaging (DTI) tractography approaches[16, 17]. Graph theoretical analysis suggested that WM networks characterized many important topological organizations, such as small-worldness[18]. To our knowledge, no studies reported the topological differences of WM networks in ESRD patients with SHPT and without SHPT.

In this study, we hypothesized that the topological organization of the WM structural network was altered in ESRD patients with peritoneal dialysis, and we further detected the relationship between the neuropsychological scores and clinical biomarkers with network metrics. For this hypothesis, we included various physiological data from 50 patients with ESRD and 25 healthy controls, including cognitive test, laboratory examinations and DTI data. We used DTI tractography and graph theory methods to detect changes in the topological organization of the WM structural networks in ESRD patients with SHPT, without SHPT and healthy controls. The correlation analyzes among network topographical organizations, global cognitive scores and clinical biomarkers were taken.

Methods And Materials

Participants

The present study was approved by the Ethics committee of the Second Hospital of Anhui Medical University and all participants obtained written informed consent. Fifty hemodialysis ESRD patients (25 patients with SHPT, 14 males and 11 females, mean age 42.20±7.53 year (SHPT group); 25 patients without SHPT, 15 males and 10 females, mean age 41.96±6.17 year (Non-SHPT group)) from the nephrology department in Second hospital of Anhui Medical University between January 2017 and July 2018. All subjects were right-handed and complete the neuropsychological test. The inclusion criteria as following: (1) clinically diagnosed ESRD (estimated glomerular filtration rate eGFR less than 15 mL/min/1.73m2), (2) receiving regular hemodialysis three times a week at our hospital, and (3) more than 18 years older. Exclusion criteria were as following: (1) obviously encephalopathy revealed by clinician or image investigation, (2) neurologic complications of ESRD treatment, (3) any history of drug/alcohol abuse, (4) leukoencephalopathy on previous MRI, and (5) MRI contraindication.

In addition, 25 healthy right-handed controls (12 males and 13 females, mean age 41.80±7.15 year (HC group)) without history of neurologic, psychiatric, and traumatic diseases were recruited from the local community. All healthy controls had no kidney disease and did not perform laboratory test.

Neuropsychological test

Before the MRI scan, we used Montreal Cognitive Assessment (MoCA) to assess the participants' global cognitive abilities. It with a score less than 26 was diagnose of cognitive impairment[19].

Laboratory test

Laboratory tests were detected in all patients to evaluate their renal function, serum creatinine, and urea levels within 24h prior to MRI scan.

MRI Acquisition

MR imaging data were acquired with a 3.0T Siemens scanner in the Second Hospital of Anhui Medical University. All subjects were placed in a standard head coil. Foam padding was used to reduce head motion and scanner noise. We obtained 3D high resolution T1 weighted structural images (TE/TR=2.98/1900ms, FOV=256×256, slice thickness=1mm, voxel size=1×1×1mm3, number of slices=176) and diffusion weighted images (TE/TR=84/8400ms, FOV=256×256, slice thickness=3mm, slice gap=0, b=0,1000 s/mm2, direction=30) in all subjects. All subjects were told to remain still, keep their eyes closed and stay awake during the entirety of the MRI scan.

Data Processing

The data preprocessing and network construction were performed by PANDA (www.nitrc.org/projects/panda), which is a pipeline toolbox for diffusion MRI analysis[20]. Briefly, the image preprocessing consisted of several steps: format conversion of original data (DICOM), BET (skull removal), eddy current and head motion correction, fractional anisotropy (FA) calculation, diffusion tensor tractography.

WM network construction

Network node definition. The structural images of each individual participant were firstly co-registered to their first b0 images and resliced into the DTI space by linear transformation. Then, the resliced structural images were non-linearly normalized to the MNI space. Finally, the derived deformation parameters were inverted and employed to warp the automated anatomical labeling (AAL) atlas[21] from the MNI space to diffusion image native space. After this procedure, 90 cortical and subcortical regions (45 for each hemisphere) were obtained, each representing a network node[18] (Table 1, Figure 1).

Network edge definition. To define the edges of structural network, we select a threshold value for the fiber bundles (with end-points in both nodes during the fiber tracking). To reduce false positive connections due to limited resolution of DTI when a minimum of three fibers as a threshold[22]. The fiber number (FN) of the connected fibers between two regions as the weights of the network edges. Finally, the FN weighted structural networks were constructed for each participant, which was represented by a symmetric 90×90 matrix[23] (Figure 1).

Network analysis

The WM network topological properties were analyzed using graph theory by GRETNA (www.nitrc.org/projects/gretna). To characterize the topological organization of WM structural network, several key measures were considered. They are the clustering coefficient (Cp), shortest path length (Lp), small-worldness (σ) (normalized clustering coefficient (γ) and normalized shortest path length (λ)), local efficiency (Eloc), and global efficiency (Eg). The Cp of a network is the average of the clustering

coefficient of each node in the network, which indicates the local efficiency for the transformation of the information. The Lp of the entire network refers to the average shortest travel distance across all nodes and indicates the most efficiency information transfer between the two nodes.

To examine the γ and λ in this study, we generated 100 matched random networks which had the same number of nodes, edges, and degree distribution, but preserved the weighted distribution of the real network. We computed the γ (γ=Cp/Cprandom) and λ (λ=Lp/Lprandom), where Cprandom and Lprandom are the average clustering coefficient and shortest path length over the random network, respectively. A small world network should meet the γ is much larger than 1 and λ is close to 1.

Eg is the average of the inverse of the shortest path length of all node pairs in the network and usually reflects the ability of the network in parallel information processing. Eloc is the average of the global efficiency of the community neighboring all nodes in the network and represents the fault tolerance level of the network.

Identification of Hubs

Hubs of structural networks are essential nodes that are identified in various ways. In the present study, we applied regional efficiency to identify the hubs of the network. A node is considered as a hub if its regional efficiency is at least one SD greater than the mean nodal efficiency of the network.

Statistical analysis

Demographic and clinical data were analyzed using SPSS 23.0. Group differences in age, education and neuropsychological tests were used by one-way analysis of variance (ANOVA). Post hoc pairwise comparisons were then performed using t test. The gender data were analyzed by chi-square test. In addition, two-sample t test compared clinical data between two patients' group.

For group effects in global and regional network metrics, comparisons were conducted among three groups by one-way ANOVA. Levels of significance were set at $p<0.05$ and a Bonferroni correction for multiple testing was applied for group differences (α=0.05/3=0.017). We also detected the relationship between network metrics and neuropsychological test scores and clinical index by correlation analysis. To investigate the correlation between neuropsychological test scores and specific brain regions, the nodes with significant group differences were taken.

Results

Neuropsychological and Clinical Assessments

The demographic, neuropsychological, and clinical data of the study are shown in Table 2. There were no significant differences in age, sex, and education among the three groups ($p>0.05$). No significant differences were found in disease duration and blood biochemistry between two groups ($p>0.05$) except the intact parathyroid hormone (iPTH) levels ($p<0.01$). For neuropsychological test, there were significant

decreased global cognition scores in both SHPT and Non-SHPT patients compared with healthy controls (p<0.01).

Small-Worldness

All three groups showed a typical small-world organization of structural networks expressed as γ >1 and λ ≈1 (Figure 2). Compared with healthy controls, SHPT patients had a significantly decreased Cp (p=0.011). Compared with Non-SHPT patients, SHPT patients had a significantly lower γ (p=0.012) and λ (p=0.006).

Network Efficiency

Compared with healthy controls, only SHPT patients had significantly lower Eloc (p=0.010). No group difference was found for Eg. (Figure 2)

Nodal characteristics

Identification of network hubs

The regions were defined as network hubs if their nodal efficiency was 1 SD greater than the average of the network. The study identified 12 hub nodes of the WM structural networks in HC group, and 14 hub nodes in both SHPT and Non-SHPT group. In three groups, 11 hub regions were identified in common, including the bilateral precental gyrus (PreCG), bilateral supplementary motor area (SMA), bilateral precuneus (PCUN), right dorsolateral superior frontal gyrus (SFGdor), right middle frontal gyrus (MFG), right median cingulate and paracingulate gyri (DCG), left postcentral gyrus (PoCG) and right putamen (PUT). One hub region, the right middle temporal gyrus (MTG), was identified as a hub in HC group. In addition, left PUT was identified as a hub in both SHPT and Non-SHPT group. Two brain regions, left middle frontal gyrus (MFG) and right PoCG, were identified as hubs in the SHPT group but not in Non-SHPT group. However, left DCG and left middle occipital gyrus (MOG) were identified hubs in Non-SHPT group (Figure 3).

Between-group difference in regional efficiency

We further localized the regions with altered nodal efficiency in ESRD patients (Figure 4, table 3). Among three groups, we found regions with the most significant decreased were mainly distributed in the frontal and parietal cortices, including 5 frontal regions (bilateral SMA, left PreCG, left MFG and right ROL), 3 parietal regions (bilateral PoCG and right SMG), 2 temporal regions (bilateral MTG) and 2 subcortical regions (right THA and right PUT). Post hoc tests showed that all these regions had a reduced efficiency in both SHPT and Non-SHPT group compared with HC. Moreover, 8 of these regions, including 2 frontal regions (left PreCG and left MFG), 3 parietal regions (bilateral PoCG and right SMG), 1 temporal region (right MTG) and 2 subcortical regions (right THA and right PUT) showed significantly reduced efficiency in Non-SHPT group as compared with SHPT group.

Correlations between network metrics and Neuropsychological tests and clinical data

We performed the correlation between network metrics and global cognition scores and clinical data. It was found that the iPTH and Lp was significantly negatively correlated with global cognition scores in ESRD patients (r=-0.531, p=0.000, r=-0.289, p=0.042, respectively). For clinical data, we found that iPTH level was significantly negatively correlated with γ (r=-0.351, p=0.013), λ (r=-0.407, p=0.003) and σ (r=-0.328, p=0.020) (Figure 5). For nodal efficiency, we conducted only the nodes in the abnormal regions (12 regions in Table 3). We did not find the correlation between nodal efficiency and global cognition scores and clinical index in these regions.

Discussion

The present study showed the topological alterations of WM networks in ESRD patients with SHPT by using DTI tractography and graph theory methods. The main findings are as follows: 1) decreased Cp in SHPT group, 2) lower Eloc for SHPT patients, 3) alterations in γ, λ and σ between two patients' group, 4) alterations in nodal efficiency in two patients' group; 5) correlation between network metrics and neuropsychological tests and clinical data. These results help us understanding the neurophysiological mechanisms in ESRD patients with SHPT and without SHPT from a network perspective.

WM network among three groups showed a typical small-world organization, although had difference of γ and λ between SHPT and Non-SHPT group, which were consistent with previous studies in healthy people[24, 25]. However, several topological properties, including Cp, Lp and Eloc were significantly altered in SHPT group compared with HC group. The fact that the WM network in SHPT patients had a lower Cp and higher Lp compared to healthy controls indicated ineffective information transmission in SHPT patients. From the perspective of network efficiency, we demonstrated a lower Eloc in SHPT patients compared to healthy controls, which suggests a loss of short-range connections throughout the brain network, likely attributable to change in the modularized information processing ability and fault tolerance in information transfer of the network[26].

Of 12 brain regions identified as hubs from healthy controls, 11 brain regions in all three groups. We found both SHPT and Non-SHPT group added two more brain regions as hubs, left MFG, right PoCG and left DCG, left MOG, respectively. On the other hand, the right MTG was no more as a hub in both SHPT and Non-SHPT group. MTG involved in several cognitive processes, language and semantic memory processing and multimodal sensory integration[27-30]. Hubs play an important role in global information transfer and seem to be more vulnerable, which since that stronger connection between hub regions leads to higher probability of damage[31]. On the other hand, this result indicate that the hub was weakened, likely related to the cognitive impairment in ESRD patients.

The spatial distribution of impaired brain regions by nodal efficiency was mainly located in the frontal and parietal cortices in ESRD patients. The node with the greatest disruption was the right THA, which is an intermediary for information processing, and the anterior and mediodorsal nucleus of THA influence memory storage and retrieval, respectively[32]. Frontal-parietal cortex lesions were considered to be impaired of attention function, such as working memory, visuo-spatial attention and attention shift[33-

35]. Some previous studies have demonstrated that ESRD patients had neuropsychological problems such as attention, learning and memory, speed and decision making[36, 37]. Moreover, ESRD patients had significantly decreased cerebral blood flow in the frontal cortex and thalamus in perfusion study[38]. In addition, several functional MRI studies have consistently shown ReHo and FC decreased in the frontal and parietal cortex in ESRD patients[39, 40]. In short, the concurrent abnormalities in functional studies and our disrupted WM connection in the same brain region could be the specific metabolic brain disorders in ESRD patients.

We first found that the MoCA scores negatively associated with Lp, and iPTH level also negatively correlated with small-world organization by two indexes (γ and λ) in ESRD patients. The small-worldness indicates an optimal balance between local specialization and global integration. The Lp and small-worldness changes reflect a possible disruption of WM connections in ESRD patients with increased iPTH level. However, we did not find the relationship between neuropsychological test and clinical data with global network measures in SHPT or Non-SHPT group, which may be attribute to a small sample size.

There are several limitations that should be addressed. First, the employment of deterministic tractography to define the WM network edges, which is insufficient in resolving fiber crossing, may result in a loss of existing fibers. Second, we only constructed WM structural networks, and the combination of the functional and structural network would need in the further studies. Third, we performed MoCA test for global cognitive, detailed and battery of neuropsychological tests of cognitive function is needed.

In conclusion, our results indicated that brain structural connectome in ESRD patients with SHPT was more disrupted than without SHPT patients, so as cognitive impairment. The iPTH level may a risk factor for cognitive impairment in ESRD patients and WM structure network has the potential connectome-based biomarkers for early detection.

Declarations

Conflict of interest

The authors declare no conflict of interest.

Funding:

This work was supported by Anhui Provincial Public Linkage Projects (1604f0804025), University natural science research project of Anhui province (KJ2018A0201), Anhui Provincial General Medicine Clinical Scientific Projects (2016QK089) and Science research foundation of Anhui medical university(2017xkj037).

Reference

[1] Bugnicourt JM, Godefroy O, Chillon JM, Choukroun G, Massy ZA. Cognitive disorders and dementia in CKD: the neglected kidney-brain axis. Journal of the American Society of Nephrology : JASN 2013;24(3):353-63.

[2] Liu ZH. Nephrology in china. Nature reviews Nephrology 2013;9(9):523-8.

[3] Kurella M, Chertow GM, Luan J, Yaffe K. Cognitive impairment in chronic kidney disease. Journal of the American Geriatrics Society 2004;52(11):1863-9.

[4] Jorde R, Waterloo K, Saleh F, Haug E, Svartberg J. Neuropsychological function in relation to serum parathyroid hormone and serum 25-hydroxyvitamin D levels. The Tromso study. Journal of neurology 2006;253(4):464-70.

[5] Seifter JL, Samuels MA. Uremic encephalopathy and other brain disorders associated with renal failure. Seminars in neurology 2011;31(2):139-43.

[6] Theofilou P. Quality of life in patients undergoing hemodialysis or peritoneal dialysis treatment. Journal of clinical medicine research 2011;3(3):132-8.

[7] Lee SY, Lee HJ, Kim YK, Kim SH, Kim L, Lee MS, et al. Neurocognitive function and quality of life in relation to hematocrit levels in chronic hemodialysis patients. Journal of psychosomatic research 2004;57(1):5-10.

[8] Drueke TB, Locatelli F, Clyne N, Eckardt KU, Macdougall IC, Tsakiris D, et al. Normalization of hemoglobin level in patients with chronic kidney disease and anemia. The New England journal of medicine 2006;355(20):2071-84.

[9] Singh AK, Szczech L, Tang KL, Barnhart H, Sapp S, Wolfson M, et al. Correction of anemia with epoetin alfa in chronic kidney disease. The New England journal of medicine 2006;355(20):2085-98.

[10] Chou FF, Chen JB, Hsieh KC, Liou CW. Cognitive changes after parathyroidectomy in patients with secondary hyperparathyroidism. Surgery 2008;143(4):526-32.

[11] Kim SM, Zhao D, Schneider ALC, Korada SK, Lutsey PL, Guallar E, et al. Association of parathyroid hormone with 20-year cognitive decline: The ARIC study. Neurology 2017;89(9):918-26.

[12] Lee CB, Yu SH, Kim NY, Kim SM, Kim SR, Oh SJ, et al. Association Between Coffee Consumption and Circulating Levels of Adiponectin and Leptin. Journal of medicinal food 2017;20(11):1068-75.

[13] Pi HC, Xu YF, Xu R, Yang ZK, Qu Z, Chen YQ, et al. Cognitive Impairment and Structural Neuroimaging Abnormalities Among Patients with Chronic Kidney Disease. Kidney & blood pressure research 2016;41(6):986-96.

[14] Kuriyama N, Mizuno T, Ohshima Y, Yamada K, Ozaki E, Shigeta M, et al. Intracranial deep white matter lesions (DWLs) are associated with chronic kidney disease (CKD) and cognitive impairment: a 5-year follow-up magnetic resonance imaging (MRI) study. Archives of gerontology and geriatrics 2013;56(1):55-60.

[15] Luo S, Qi RF, Wen JQ, Zhong JH, Kong X, Liang X, et al. Abnormal Intrinsic Brain Activity Patterns in Patients with End-Stage Renal Disease Undergoing Peritoneal Dialysis: A Resting-State Functional MR Imaging Study. Radiology 2016;278(1):181-9.

[16] Kim JH, Choi NK, Kim SM. A Retrospective Study of Association between Peg-shaped Maxillary Lateral Incisors and Dental Anomalies. The Journal of clinical pediatric dentistry 2017;41(2):150-3.

[17] Kalaitzidis RG, Karasavvidou D, Tatsioni A, Balafa O, Pappas K, Spanos G, et al. Risk factors for cognitive dysfunction in CKD and hypertensive subjects. International urology and nephrology 2013;45(6):1637-46.

[18] Bullmore E, Sporns O. Complex brain networks: graph theoretical analysis of structural and functional systems. Nature reviews Neuroscience 2009;10(3):186-98.

[19] Nasreddine ZS, Phillips NA, Bedirian V, Charbonneau S, Whitehead V, Collin I, et al. The Montreal Cognitive Assessment, MoCA: a brief screening tool for mild cognitive impairment. Journal of the American Geriatrics Society 2005;53(4):695-9.

[20] Cui Z, Zhong S, Xu P, He Y, Gong G. PANDA: a pipeline toolbox for analyzing brain diffusion images. Frontiers in human neuroscience 2013;7:42.

[21] Tzourio-Mazoyer N, Landeau B, Papathanassiou D, Crivello F, Etard O, Delcroix N, et al. Automated anatomical labeling of activations in SPM using a macroscopic anatomical parcellation of the MNI MRI single-subject brain. NeuroImage 2002;15(1):273-89.

[22] Zou L, Su L, Qi R, Bao F, Fang X, Wang L, et al. Abnormal topological organization in white matter structural networks in survivors of acute lymphoblastic leukaemia with chemotherapy treatment. Oncotarget 2017;8(36):60568-75.

[23] Zhao T, Cao M, Niu H, Zuo XN, Evans A, He Y, et al. Age-related changes in the topological organization of the white matter structural connectome across the human lifespan. Human brain mapping 2015;36(10):3777-92.

[24] Gong G, He Y, Concha L, Lebel C, Gross DW, Evans AC, et al. Mapping anatomical connectivity patterns of human cerebral cortex using in vivo diffusion tensor imaging tractography. Cerebral cortex 2009;19(3):524-36.

[25] Gong G, Rosa-Neto P, Carbonell F, Chen ZJ, He Y, Evans AC. Age- and gender-related differences in the cortical anatomical network. The Journal of neuroscience : the official journal of the Society for

Neuroscience 2009;29(50):15684-93.

[26] Achard S, Bullmore E. Efficiency and cost of economical brain functional networks. PLoS computational biology 2007;3(2):e17.

[27] Siddarth P, Burggren AC, Eyre HA, Small GW, Merrill DA. Sedentary behavior associated with reduced medial temporal lobe thickness in middle-aged and older adults. PloS one 2018;13(4):e0195549.

[28] Deshpande AK, Tan L, Lu LJ, Altaye M, Holland SK. fMRI as a Preimplant Objective Tool to Predict Children's Postimplant Auditory and Language Outcomes as Measured by Parental Observations. Journal of the American Academy of Audiology 2018;29(5):389-404.

[29] Puschmann S, Thiel CM. Changed crossmodal functional connectivity in older adults with hearing loss. Cortex; a journal devoted to the study of the nervous system and behavior 2017;86:109-22.

[30] Nilakantan AS, Voss JL, Weintraub S, Mesulam MM, Rogalski EJ. Selective verbal recognition memory impairments are associated with atrophy of the language network in non-semantic variants of primary progressive aphasia. Neuropsychologia 2017;100:10-7.

[31] Crossley NA, Mechelli A, Scott J, Carletti F, Fox PT, McGuire P, et al. The hubs of the human connectome are generally implicated in the anatomy of brain disorders. Brain : a journal of neurology 2014;137(Pt 8):2382-95.

[32] Van der Werf YD, Jolles J, Witter MP, Uylings HB. Contributions of thalamic nuclei to declarative memory functioning. Cortex; a journal devoted to the study of the nervous system and behavior 2003;39(4-5):1047-62.

[33] Smith R, Lane RD, Alkozei A, Bao J, Smith C, Sanova A, et al. Maintaining the feelings of others in working memory is associated with activation of the left anterior insula and left frontal-parietal control network. Social cognitive and affective neuroscience 2017;12(5):848-60.

[34] Heinen K, Feredoes E, Ruff CC, Driver J. Functional connectivity between prefrontal and parietal cortex drives visuo-spatial attention shifts. Neuropsychologia 2017;99:81-91.

[35] Mastroberardino S, Santangelo V, Macaluso E. Crossmodal semantic congruence can affect visuo-spatial processing and activity of the fronto-parietal attention networks. Frontiers in integrative neuroscience 2015;9:45.

[36] Raphael KL, Wei G, Greene T, Baird BC, Beddhu S. Cognitive function and the risk of death in chronic kidney disease. American journal of nephrology 2012;35(1):49-57.

[37] Giang LM, Weiner DE, Agganis BT, Scott T, Sorensen EP, Tighiouart H, et al. Cognitive function and dialysis adequacy: no clear relationship. American journal of nephrology 2011;33(1):33-8.

[38] Fazekas G, Fazekas F, Schmidt R, Flooh E, Valetitsch H, Kapeller P, et al. Pattern of cerebral blood flow and cognition in patients undergoing chronic haemodialysis treatment. Nuclear medicine communications 1996;17(7):603-8.

[39] Liang X, Wen J, Ni L, Zhong J, Qi R, Zhang LJ, et al. Altered pattern of spontaneous brain activity in the patients with end-stage renal disease: a resting-state functional MRI study with regional homogeneity analysis. PloS one 2013;8(8):e71507.

[40] Zheng G, Wen J, Zhang L, Zhong J, Liang X, Ke W, et al. Altered brain functional connectivity in hemodialysis patients with end-stage renal disease: a resting-state functional MR imaging study. Metabolic brain disease 2014;29(3):777-86.

Tables

Table 1. Cortical and subcortical regions of interest defined in the study.

Index	Regions	Abbreviation	Index	Regions	Abbreviation
(1,2)	Precental gyrus	PreCG	(47,48)	Lingual gyrus	LING
(3,4)	Superior frontal gyrus, dorsolateral	SFGdor	(49,50)	Superior occipital gyrus	SOG
(5,6)	Superior frontal gyrus, orbital part	ORBsup	(51,52)	Middle occipital gyrus	MOG
(7,8)	Middle frontal gyrus	MFG	(53,54)	Inferior occipital gyrus	IOG
(9, 10)	Middle frontal gyrus, orbital part	ORBmid	(55,56)	Fusiform gyrus	FFG
(11,12)	Inferior frontal gyrus, opercular part	IFGoperc	(57,58)	Postcentral gyrus	PoCG
(13,14)	Inferior frontal gyrus, triangular part	IFGtriang	(59,60)	Superior parietal gyrus	SPG
(15,16)	Inferior frontal gyrus, orbital part	ORBinf	(61,62)	Inferior parietal, but supramarginal and angular gyri	IPL
(17,18)	Rolandic operculum	ROL	(63,64)	Supramarginal gyrus	SMG
(19,20)	Supplementary motor area	SMA	(65,66)	Angular gyrus	ANG
(21,22)	Olfactory cortex	OLF	(67,68)	Precuneus	PCUN
(23,24)	Superior frontal gyrus, medial	SFGmed	(69,70)	Paracentral lobule	PCL
(25,26)	Superior frontal gyrus, medial orbital	ORBsupmed	(71,72)	Caudate nucleus	CAU
(27,28)	Gyrus rectus	REC	(73,74)	Lenticular nucleus, putamen	PUT
(29,30)	Insula	INS	(75,76)	Lenticular nucleus, pallidium	PAL
(31,32)	Anterior cingulate and paracingulate gyri	ACG	(77,78)	Thalamus	THA
(33,34)	Median cingulate and paracingulate gyri	DCG	(79,80)	Heschl gyrus	HES
(35,36)	Posterior cingulate gyrus	PCG	(81,82)	Superior temporal gyrus	STG
(37,38)	Hippocampus	HIP	(83,84)	Temporal pole: superior temporal gyrus	TPOsup
(39,40)	Parahippocampal gyrus	PHG	(85,86)	Middle temporal gyrus	MTG
(41,42)	Amygdala	AMYG	(87,88)	Temporal pole: middle temporal gyrus	TPOmid
(43,44)	Calcarine fissure and surrounding cortex	CAL	(89,90)	Inferior temporal gyrus	ITG
(45,46)	Cuneus	CUN			

Table 2. Demographic characteristics of study participants.

Characteristics	SHPT(n=25)	Non-SHPT(n=25)	Healthy Controls(n=25)	*P*-value
Age (year)	42.20±7.53	42.95±6.39	41.80±7.15	0.98[a]
Gender (M/F)	14/11	15/10	12/13	0.69[b]
Education(year)	9.36±2.86	9.44±3.23	11.12±2.54	0.06[a]
Disease duration(month)	40.76±18.28	38.44±16.84	-	0.64[c]
Urea(mmol/L)	26.14±7.08	26.01±8.06	-	0.95[c]
Creatinine(μmol/L)	962.96±212.19	914.48±274.11	-	0.49[c]
Uric acid(μmol/L)	447.04±38.42	463.00±52.40	-	0.23[c]
Calcium(mmol/L)	2.37±0.33	2.25±0.20	-	0.14 [c]
Phosphate (mmol/L)	1.26±0.12	1.27±0.10	-	0.74 [c]
Vitamin D (ng/ml)	8.75±4.62	11.14±4.09	-	0.06 [c]
iPTH(pg/mL)	1401±721.06	35.68±11.01	-	0.00[c]
MoCA(score)	22.92±2.22	24.96±1.59	28.00±1.22	0.00[a*#]

Note: a *p* value from one-way analysis of variance (ANOVA), b *p* value from chi-square test, c *p* value from t test. * means the post hoc analysis showed significant group difference between SHPT and Healthy controls. # means the post hoc analysis showed significant group difference between Non-SHPT and Healthy controls

Table3. Brain regions with significant group effects in nodal efficiency among SHPT, Non-SHPT patients and healthy controls.

Regions	F value of ANOVA(p value)	p value of post hoc test		
		SHPT versus healthy controls	Non-SHPT versus healthy controls	SHPT versus Non-SHPT
THA.R	26.51(0.000)	0.000	0.000	0.003
SMA.L	22.74(0.000)	0.000	0.000	0.341
SMA.R	22.66(0.000)	0.000	0.000	0.363
MTG.R	22.09(0.000)	0.000	0.000	0.039
PreCG.L	19.20(0.000)	0.002	0.000	0.004
PoCG.L	17.44(0.000)	0.005	0.000	0.004
SMG.R	16.67(0.000)	0.001	0.000	0.035
MFG.L	16.36(0.000)	0.008	0.000	0.004
ROL.R	15.57(0.000)	0.000	0.000	0.097
MTG.L	14.56(0.000)	0.000	0.000	0.285
PoCG.R	14.14(0.000)	0.044	0.000	0.002
PUT.R	13.99(0.000)	0.009	0.000	0.012

Figures

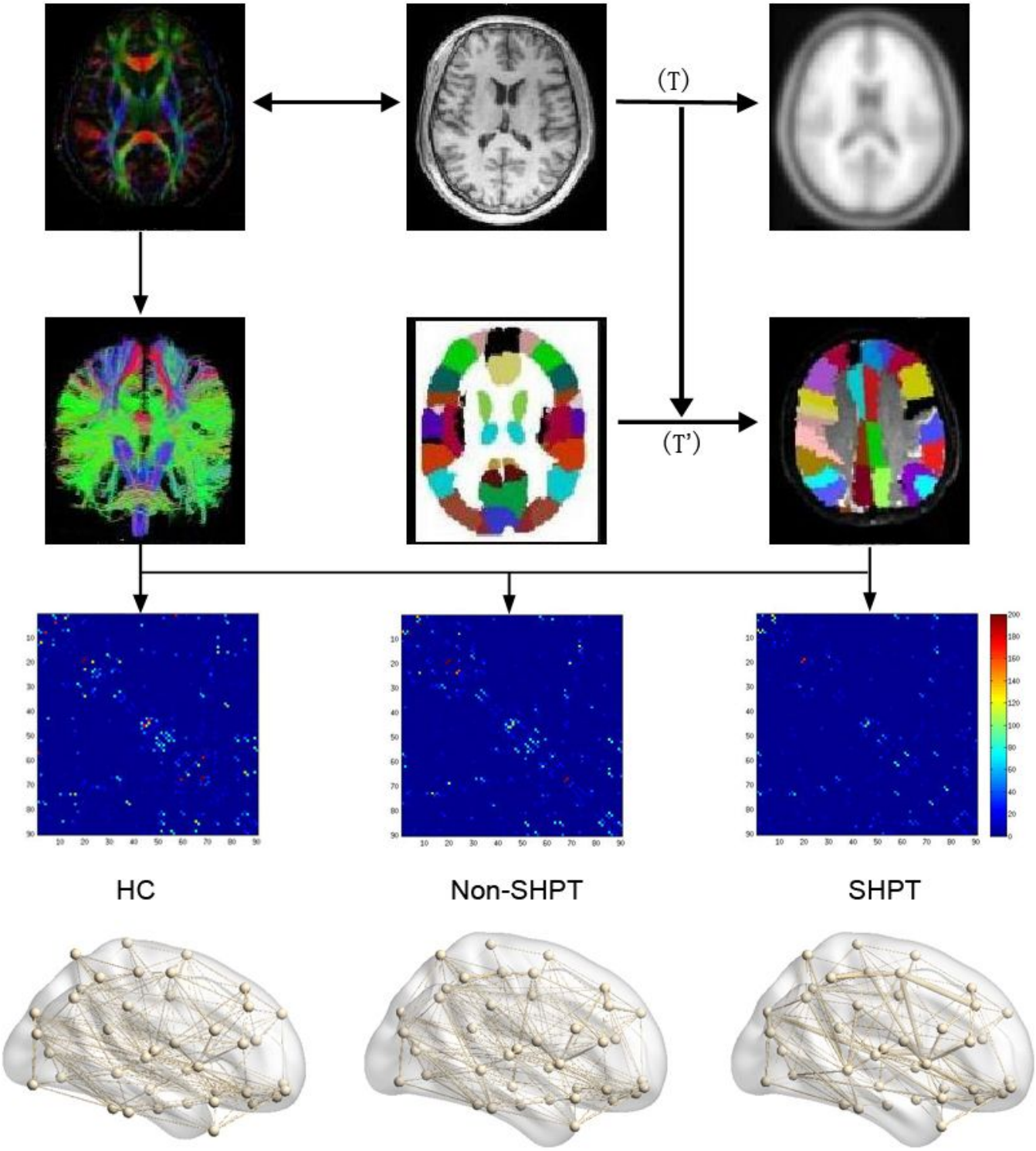

Figure 1

Flowchart for the construction of WM structural network by DTI. 1) The rigid coregisteration from T1-weighted image to the DTI native space. 2) The nonlinear registration from the resultant T1 image to the ICBM152 T1 template in the MNI space resulting a transformation matrix (T). 3) The application of the inverse transformation (T') to the AAL template in the MNI space, resulting in the subject-specific AAL mask in the DTI native space. 4) The whole brain WM fibers were reconstructed by DTI deterministic

tractography method. 5) The fiber number (FN) weighted networks of each subject were created by computing FN that connected each pair of brain regions. The matrices and 3D representations (lateral view) of the mean WM structural network of each group are shown in the bottom panel. The nodes and edges were mapped onto the cortical surfaces by BrainNet viewer software. HC, healthy controls, Non-SHPT, end-stage renal disease (ESRD) without secondary hyperparathyroidism (SHPT) patients, SHPT, ESRD with SHPT patients.

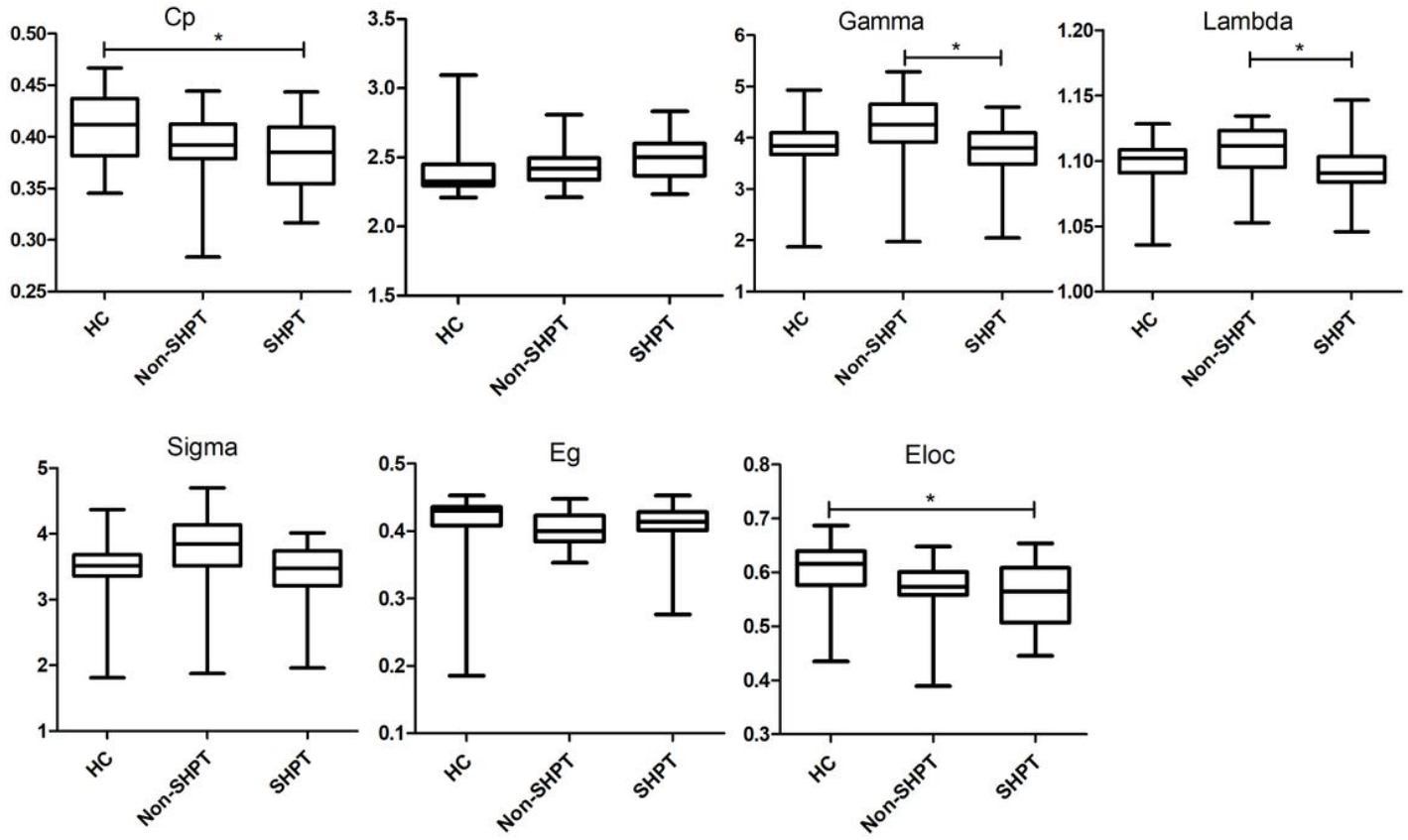

Figure 2

Boxplot shows the difference in global topological measures among the three group (medical, 50th percentile values, minimum and maximum). Significant differences were observed in Cp, Lp and Eloc between HC and SHPT group. Significant group effects were found in σ by two indexes (γ and λ) between Non-SHPT and SHPT group. *P<0.05.

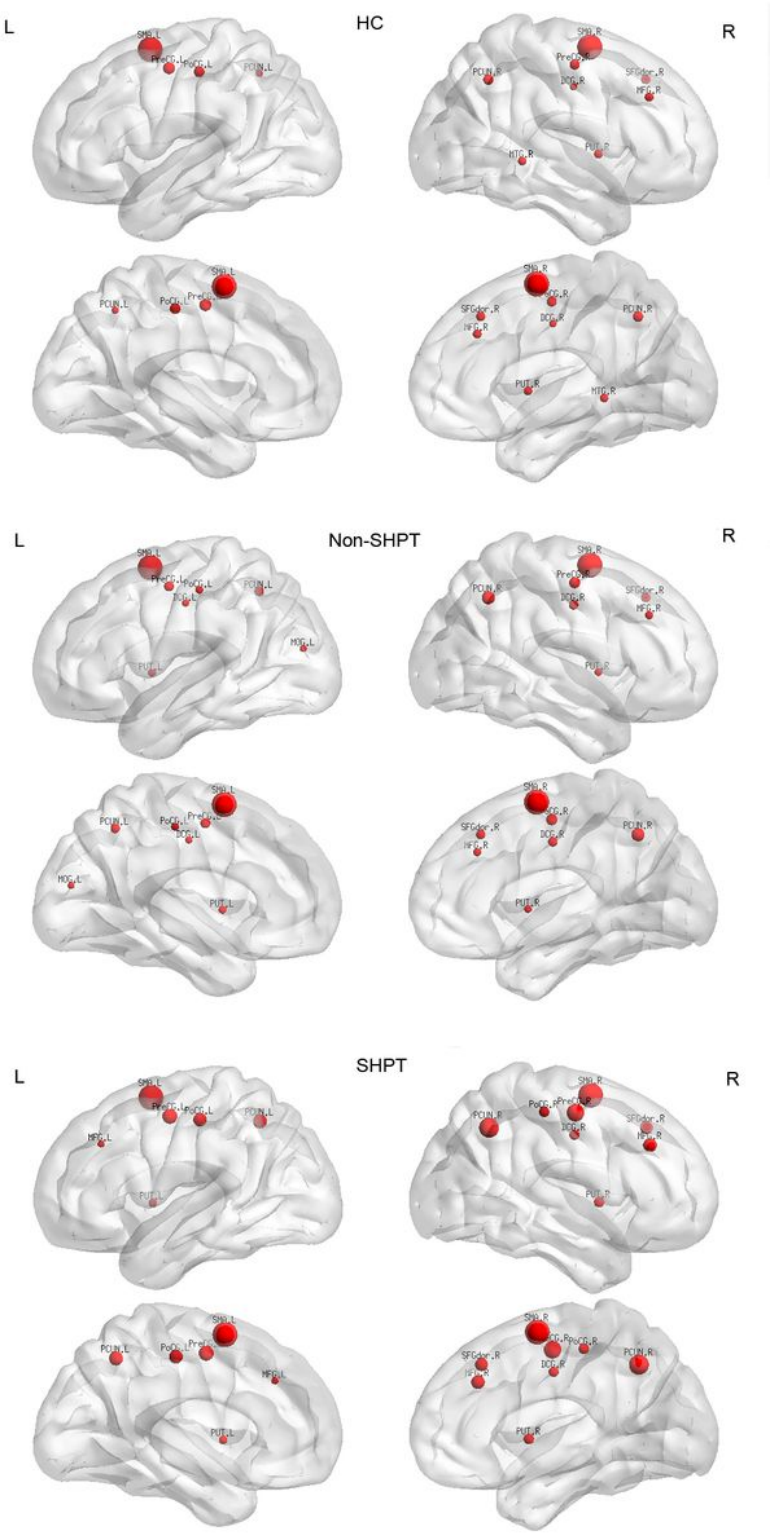

Figure 3

The global network hubs with nodal efficiency in HC, Non-SHPT and SHPT group. HC, healthy control, Non-SHPT, end-stage renal disease (ESRD) without secondary hyperparathyroidism (SHPT) patients, SHPT, ESRD with SHPT patients.

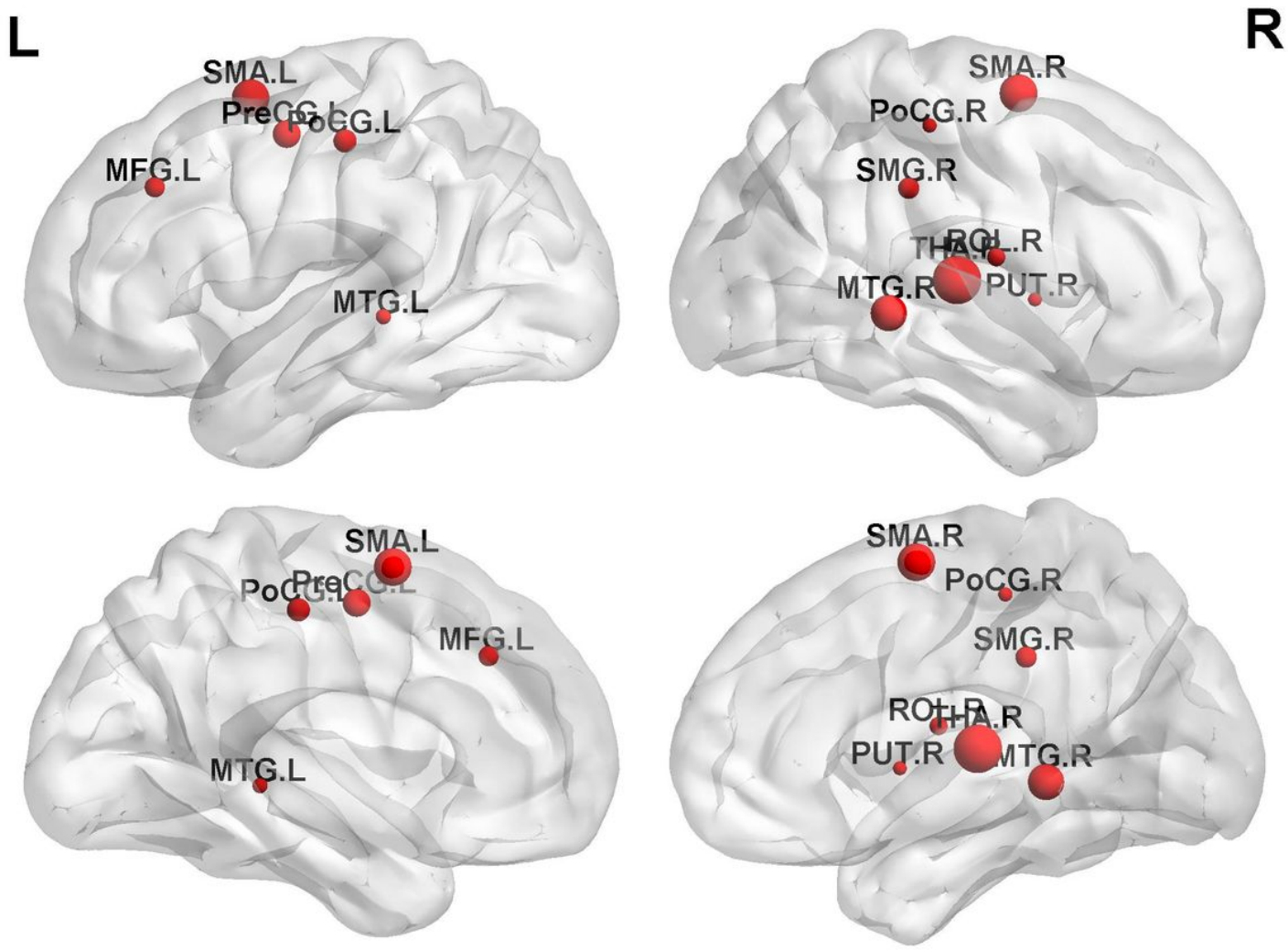

Figure 4

The distribution of brain regions with significant group difference in the nodal efficiency among three group. The node size represents the significance of between-group differences.

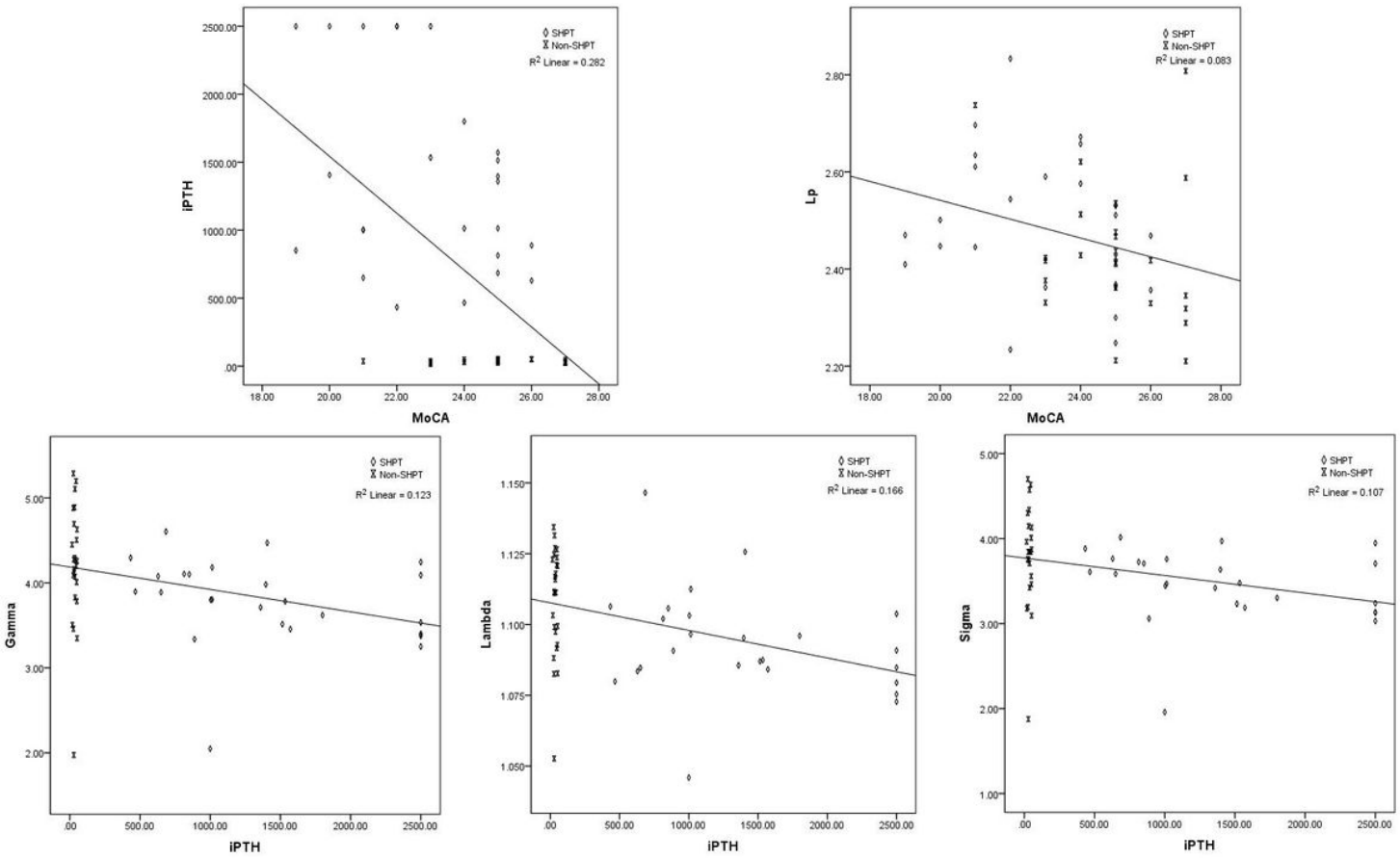

Figure 5

Scatterplots of correlation between network metrics and global cognition scores and clinical data.